MALAYSIAN JOURNAL OF SCIENCE
MJS
ISSN 1394 - 3065

FAST-UTHM Global Nexus Conference 2024
Special issue

Malaysian Journal of Science 45 (Special Issue 1): 1-10 (June 2026)
https://mjs.um.edu.my

Surface Temperature and Pressure Drop Simulation Analysis of Nanofluid Flow in Microchannel Heat Sink

Nurafiqah Mohd Alhata[1a], Amira Saryati Ameruddin[2a]*, Rosmila Abdul-Kahar[3a] and Mirza Basyir Rodhuan[4a]

Abstract: The increasing demand for high-performance electronic devices has driven the need more effective thermal management solutions. Standard air-cooling methods fall short when handling high heat flow rates. Among the most promising solutions is the Micro Channel Heat Sink (MCHS), specifically designed to address this challenge. To draw heat away from the chip, a cold liquid navigates intricate channels within the electronic system. The design of the heat sink profoundly influences crucial factors, such as microchannel area, heatsink size, channel width, height, and inlet/outlet diameters, each of which is affected differently by the heat sink's configuration. This study investigated heat transfer performance across various thicknesses, exploring nanoliquids, air, and water as cooling agents. After reviewing the setup steps, the ideal fluid performance for the given design is identified. Using COMSOL Multiphysics 5.5 software, a 3D model of a rectangular copper MCHS is created employing the finite element method. Results indicate that a 5 mm channel thickness using Aluminum oxide (Al_2O_3) nanofluids yields the most promising thickness based on the findings. Al_2O_3 exhibits outstanding performance, maintaining momentum even at lower temperatures. The influence of fluid flow velocity on the MCHS is reflected in the 5 mm channel thickness, significantly impacting the effective pressure drop. One avenue for potentially enhancing performance involves considering the aspect ratio of nanofluidic particles and exploring diverse materials such as iron and aluminum.

Keywords: Nanofluid, Heat transfer, Temperature, Pressure drop, Microchannel heat sink

1. Introduction

MCHS have emerged as pivotal components for cooling high-performance electronic devices since their inception by Tuckerman and Pease (1981). Traditional air-cooling methods struggle to handle the high heat generated by modern devices, prompting the search for more effective cooling techniques. Liquid cooling through MCHS, where chilled liquid flows through tiny channels to remove heat from the chip, has proven to be one of the most efficient solutions (Van Oevelen, 2014). These channels are built into the heat sink, which is placed on or embedded within the chip to ensure optimal cooling. MCHS are typically made from highly conductive materials, such as copper and aluminum. Copper has better thermal conductivity, while aluminum is lighter and more affordable. Many designs use both materials to balance performance, weight, and cost, ensuring efficient cooling of electronic devices.

One of the main challenges in optimizing MCHS is enhancing heat transfer efficiency. Adjusting the shape, size, and orientation of the microchannels can significantly improve heat transfer and reduce pressure drop. For example, triangular fins are more effective at transferring heat than rectangular ones, although specific designs, such as angled ribs, improve heat transfer while increasing pressure resistance (Behnampour *et al.,* 2017; Liou, Chang, & Chan, 2018). In addition, the size of the channels and the inlet/outlet ports also play a crucial role in thermal efficiency. Numerical simulations help engineers analyze these variables, allowing them to optimize designs for better performance without increasing costs (Dhaiban & Hussein, 2020).

Using advanced coolants, such as nanofluids, which are liquids containing tiny nanoparticles, has been shown to significantly enhance heat transfer rates. Nanofluids, such as Al_2O_3 mixed with water, can boost cooling efficiency by up to 8.58% compared to regular water (Elbadawy *et al.,* 2023). However, challenges like sedimentation and increased fluid viscosity must be addressed to ensure their long-term effectiveness (Rafiq, 2021). The performance of nanofluids is influenced by factors such as particle size, material type, and temperature. Preventing particle clumping and maintaining fluid stability over time are essential for maximizing their thermalbenefits. Ongoing research focuses on improving nanofluid stability and understanding their behavior using advanced simulations, particularly the Finite Element Method (FEM) and Computational Fluid Dynamics (CFD), which are key tools for enhancing MCHS designs (Nazzal *et al.,* 2021; Gao *et al.,* 2022).

This research used COMSOL Multiphysics software to run detailed simulations that model heat transfer and fluid flow in 3D microchannel designs. It is ideal for studying MCHS to improve cooling performance metrices. Building on earlier work by Gunnasegaran *et al.,* (2012), which demonstrated how

Authors information:
[a]Department of Physics, Faculty of Applied Sciences and Technology (FAST), Universiti Tun Hussein Onn Malaysia (UTHM), Pagoh Branch Campus, Pagoh Higher Education Hub, Km 1, Jalan Panchor, 84600 Muar, Johor Darul Ta'zim, MALAYSIA.
E-mail: gw220014@student.uthm.edu.my[1], amira@uthm.edu.my[2], ammaz5011@gmail.com[3], mirzabasyir95@gmail.com[4]

*Corresponding Author: amira@uthm.edu.my

Received: May 25, 2025
Accepted: July 30, 2025
Published: June 30, 2026

DOI: https://doi.org/10.22452/mjs.vol45sp1.1
Malaysian Journal of Science 45 (Special Issue 1): 1-10 (June 2026)

nanofluids, such as Al_2O_3 can enhance heat transfer compared to air cooling, this study extends to investigation by testing different channel thicknesses. It finds that a 5 mm thickness works best for efficient cooling and examines how fluid temperature, velocity, and novel materials, such as iron and aluminum, can enhance heat transfer. The study also explores innovative methods to enhance MCHS performance through FEM simulations.

2. Materials and method

Three key parameters must be observed in the design: heat transfer performance in solids and fluids, surface temperature, and pressure. The design in this study is adapted from research conducted by Gunnasegaran and his team (Gunnasegaran *et al.,* 2012). They focused on the 3D simulation of heat conduction, convection, and laminar flow behavior with various heat sink shapes, the effect of nanoparticle volume fraction, different types of nanofluids, and nanoparticles in different base fluids. In this paper, the heat performance of various geometry thicknesses of heat sinks and different types of nanofluids is examined. The influence of nanofluids on varying thicknesses of heat sinks is the main focus. The results are presented in terms of surface temperature and pressure.

2.1 Geometry

The inlet/outlet area, channel width, channel height, channel length, heat sink size, and copper microchannel area are the parameters examined in this study. Figure 1 shows the overall design of the inlet and outlet of the copper rectangular MCHS design in 3D. The design remain the same for the 5mm and 8mm thicknesses of the heat sink channel with different types of nanofluids. The parameter details of the MCHS design used in the simulation are shown in Table 1. Figure 2(a) and Figure 2(b) show the XZ-cut plane view and YZ-cut plane view, which were used as guidelines to present the results in the next section.

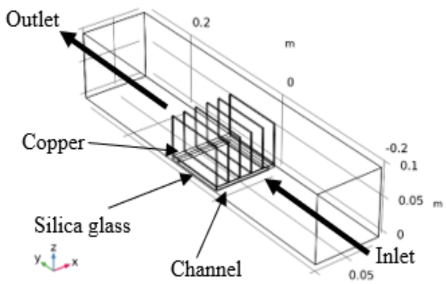

Figure 1. Copper rectangular microchannel heat sink.

Table 1. The parameters of copper rectangular microchannel heat sink.

Parameter	Dimension
Inlet/outlet area, mm	42.5 x 50
Channel width, mm	10
Channel height, mm	50
Channel length, mm	95
Microchannel area, mm^2	60 x 95

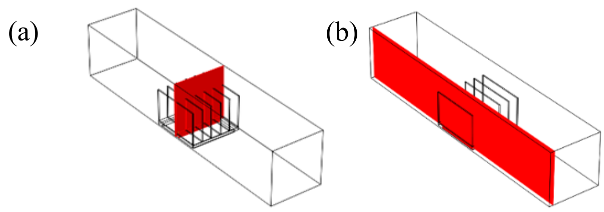

Figure 2. Microchannel heat sink (a) XZ-cut plane view and (b) YZ-cut plane view.

2.2 Nanofluids

The model design begins with an electronic chip placed at the bottom of the heat sink as a heat source made from silica glass. The copper MCHS acts as the path for nanofluids to flow and is surrounded by a domain. The physical interface is transferred from the electronic chip using nanofluids, air, and water as the fluid flows from the inlet to the outlet of the heat sink along the MCHS. As the nanofluids, air, and water flow in the rectangular channel, the thermal balance for the electronic component was optimized. In this part, the properties of all the nanofluids, air, and water were defined by inserting them into COMSOL. Thermophysical properties of solids and fluids for materials and nanofluids used in this study are shown in Tables 2 and 3.

The thermophysical properties of the solid materials and working fluids presented in Tables 2 and 3 are adapted from Patel *et al.,* (2019), Gunnasegaran *et al.,* (2012), and Mohammed *et al.,* (2010). Nanoparticle constants (Al_2O_3, SiO_2, and ZnO) and the effective nanofluid properties were determined using the conventional mixture relations described by Pak and Cho (1998) and Hamilton and Crosser (1962), validated experimentally by Sohel *et al.,* (2014) and theoretically by Malvandi and Ganji (2014). These references confirm that, for dilute nanoparticle concentrations ($\leq$ 4 vol %), the nanofluid density remains very close to that of the base fluid, differing by less than 3 %. Base-fluid properties for water and air were taken at 293 K following Patel *et al.,* (2019), Mohammed *et al.,* (2010), and the National Institute of Standards and Technology (NIST) standard property tables. The solid-phase properties of copper and silica glass were verified against those reported by Patel *et al.,* (2019) and Gunnasegaran *et al.,* (2012) to ensure consistency with established MCHS studies.

2.3 Equations

This section includes the equations of heat transfer in solids and fluids, laminar flow, temperature, pressure drop, and boundary conditions for heat transfer in solids and fluids, and laminar flow is solved in COMSOL Multiphysics. Heat transfer in solids and fluids is defined by the heat source, heat rate, heat flux, inflow, and outflow, as describe in the COMSOL Reference Manual. Eq (1) is the equation for the heat source. Inserting a value for the heat rate P_0 in the overall heat transfer rate field as

DOI: https://doi.org/10.22452/mjs.vol45sp1.1
Malaysian Journal of Science 45 (Special Issue 1): 1-10 (June 2026)

Table 2. Thermophysical properties of solid.

Thermophysical properties	Copper	Silica glass
Density, ρ_s (kg/m^3)	8690	8690
Thermal Conductivity, κ (W/m·k)	400	400
Relative Permittivity, ϵ_r	1	3.9
Heat Capacity at Constant Pressure, C_p (J/kg·k)	385	385

Table 3. Thermophysical properties of fluid.

Thermophysical properties	Al_2O_3	SiO_2	ZnO	Water	Air
Density, ρ_s (kg/m^3)	3880	2200	5600	997	1.23
Thermal Conductivity, κ (W/m·k)	30	703	113	148	0.025
Relative Permittivity, ϵ_r	8.5	3.9	5	78.3	1
Heat Capacity at Constant Pressure, C_p (J/kg·k)	791	745	495	4182	1006

mentioned in Eq (2). Q_0 as the heat per unit volume, as a linear heat source, or as a heat rate and V is the total volume.

$$Q = Q_0 \quad (1)$$

$$Q = \frac{P_0}{V} \quad (2)$$

$$U = -nU_0 \quad (3)$$

In this study, the laminar flow options available in the boundary condition options for the inlet and outlet are pressure and velocity. Eq (3) shows the normal inflow velocity, where n is the boundary normal pointing out of the domain, and U_0 is the normal inflow speed that is defined by the simulation software.

Eqs (4) and (5) are the inlet boundary conditions, and Eq (6) is the outlet boundary condition (Memon *et al.,* 2020). Below are the equations for the inlet and outlet boundary conditions:

$$T_f = T_{in} = 293K \quad (4)$$

$$u = u_{in} \quad (5)$$

$$P = P_{out} = 1atm \quad (6)$$

For the above equations, T_{in} and u_{in} are the temperature and velocity at the inlet of the heat sink. T_f is the temperature field inside the fluid. P_{out} is the pressure at the outlet. The temperature of each channel, shown in Eqs (7) and (8), was used to calculate the pressure drops along the length of the heat sink channel (Gunnasegaran *et al.,* 2012).

$$\theta = \frac{T_f - T_i}{T_w - T_i} \quad (7)$$

$$\hat{p} = \frac{\Delta P}{\rho u_{in}^2} \quad (8)$$

T_f is a fluid temperature, T_i is an inlet temperature and T_w is a wall temperature. For the Eq (8), ΔP is the pressure drop of the microchannel configuration, ρ is the water density and u_{in} is the inlet water velocity (Mohammed, Gunnasegaran, & Shuaib, 2010).

2.4 Meshing and validation

The MCHS design of the entire model used an "extremely coarse" mesh, as shown in Figure 3, to reduce computational cost while still capturing essential flow and thermal behavior, featuring 6,770 triangular and 68 vertex elements for a 2 mm channel thickness, 7,164 triangular and 68 vertex elements for 5 mm, and 6,644 triangular and 68 vertex elements for 8 mm. The minimum element quality improved from 0.114 (2 mm) to 0.2626 (5 mm) and 0.2828 (8 mm), indicating better element shapes with increasing thickness. The coarse meshing was applied because the simulation focused on broad thermal and fluid patterns, where fine local details are less critical. Boundary conditions, such as inlet/outlet flow, wall heat transfer, and symmetry, ensure realistic thermal-fluid behavior while maintaining efficient computation.

DOI: https://doi.org/10.22452/mjs.vol45sp1.1
Malaysian Journal of Science 45 (Special Issue 1): 1-10 (June 2026)

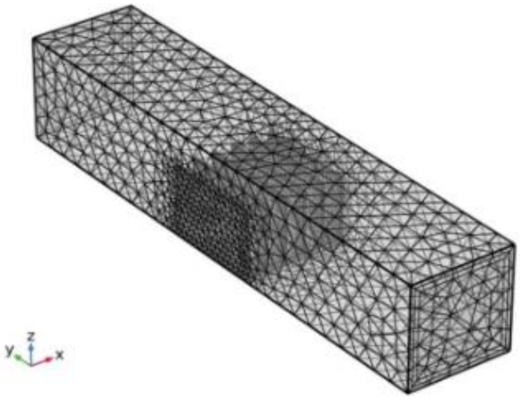

Figure 3. Meshing result by "Extremely coarse" of the model.

3. Result and discussion

This section discusses and analyzes the heat transfer performance, surface temperature, and pressure drop in a copper rectangular microchannel heat sink with varying thicknesses in Aluminum Oxide (Al2O3), Silicon Oxide (SiO2), and Zink Oxide (ZnO) nanofluids, as well as air and water. Temperature surface plots are used to present the results of temperature distributions on the boundaries of a model's geometry of the heat sink. The impact of different design conditions shows the increase or decrease in the temperature and pressure drop.

As the nanofluid passes through the heat sink channels, the heat is transferred from the electronic chip to the microchannels by conduction, convection, and radiation due to direct solid-liquid contact within the heat sink, as shown in Tables 4 and 5. The best nanofluids enhance heat removal performance at lower temperatures. The velocity of the fluid flow affects the pressure of the heat sink. According to Bernoulli's Principle, when the velocity increases, the pressure decreases. The pressure of the heat sinks changes from high to low pressure from the inlet to the outlet. The pressure drop was determined by measuring the pressure changes along the MCHS.

3.1 The effect of MCHS thickness and cooling element on the temperature and pressure surface

The copper rectangular MCHS acted as a device cooling system that enhanced the heat transfer performance while allowing nanofluids to flow along the channel. Tables 4 to 7 show the results of the temperature and pressure surface data with different nanofluids, air, and water from various views based on Figures 1, and Figure 2 (a and b).

As shown in Tables 4 and 5, the 5 mm channel, utilizing Al_2O_3 nanofluid, achieves the lowest maximum temperature of 27.39˚C, a result attributed to Al_2O_3's superior thermal conductivity, which enable efficient heat dissipation from electronic components.

Table 4. Surface temperature of microchannel heat sink from 3D view.

Nanofluids	2mm	5mm	8mm
Al_2O_3	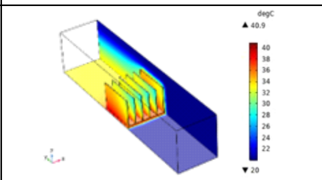	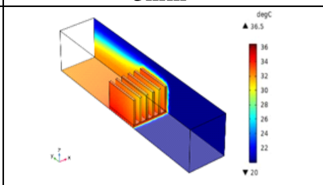	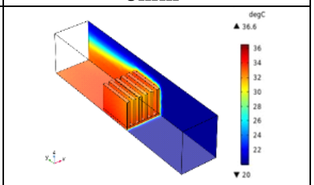
SiO_2	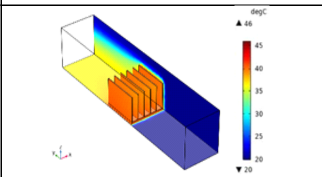	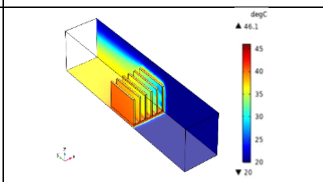	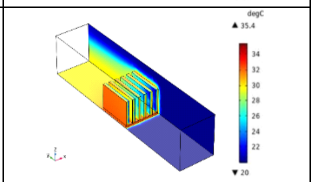
ZnO	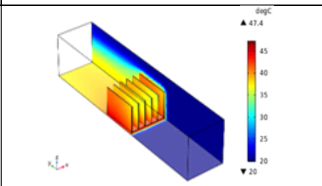	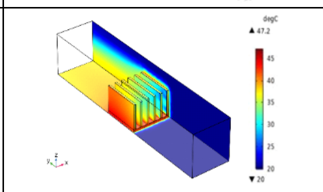	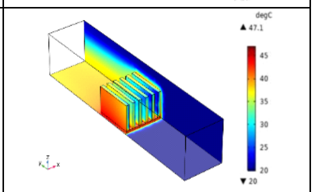
Air	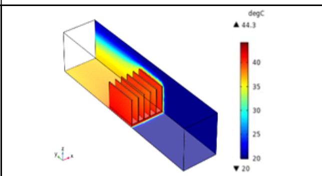	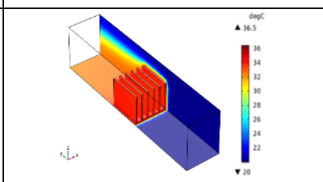	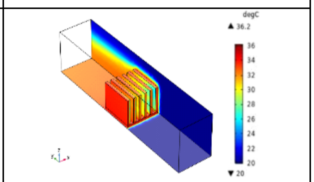
Water	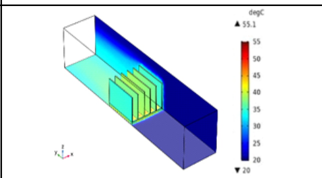	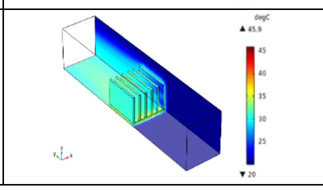	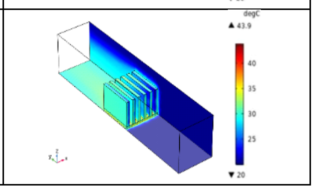

DOI: https://doi.org/10.22452/mjs.vol45sp1.1
Malaysian Journal of Science 45 (Special Issue 1): 1-10 (June 2026)

Table 5. Surface temperature of microchannel heat sink from top view.

Nanofluids	2mm	5mm	8mm
Al_2O_3	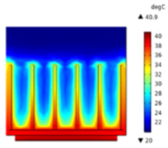	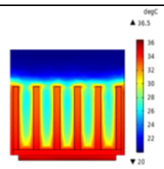	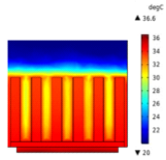
SiO_2	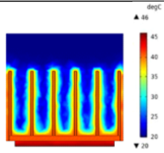	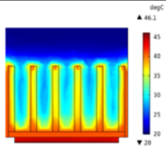	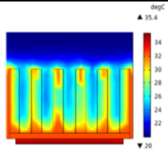
ZnO	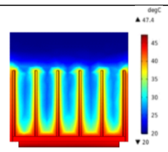	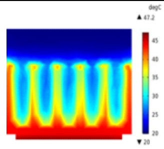	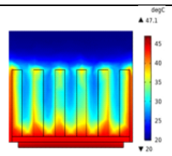
Air	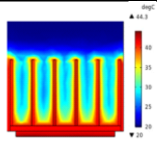	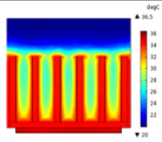	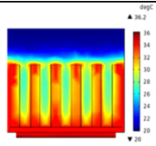
Water	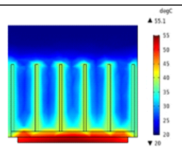	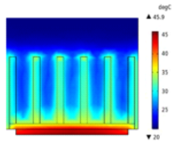	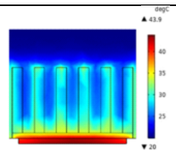

Water and ZnO in 2 mm and 8 mm channels also demonstrate effective cooling capabilities, with the lowest maximum temperatures of 27.44˚C and 29.18˚C, respectively. This performance is attributed to water's favourable flow properties and ZnO's thermal conductivity, which together improve heat removal and regulation in confined spaces.

Conversely, the 2 mm channel records the highest temperature when using ZnO nanofluid, reaching 39.52˚C. This suggests that ZnO's lower thermal conductivity restricts its performance in managing heat within narrower channels. Additionally, constrained fluid dynamics in smaller channels can further reduce effective heat absorption. Although the 8 mm channel offers a greater surface area for heat exchange, certain nanofluids, such as SiO_2, still show elevated temperatures (32.45˚C), indicating that larger channels do not consistently enhance cooling performance across all nanofluid types.

In summary, optimizing cooling performance requires careful selection of both the nanofluid and channel thickness. Nanofluids with high thermal conductivity, such as Al_2O_3, combined with appropriately sized channels, can substantially improve heat regulation in MCHS. As the fluids traverse the heat sink, temperatures decrease through conduction, convection, and radiation, with the ideal case being the lowest achievable temperature. These findings are crucial for advancing the design of heat sinks to improve the efficiency of electronic cooling systems.

Tables 6 and 7 present the results for 2 mm and 5 mm channel thicknesses from the 2D YZ-cut plane. The 8 mm channel results are shown in Table 8 for completeness. However, they are excluded from the comparative analysis as they exhibit anomalous thermal and hydraulic behavior that diverges from the consistent patterns observed for smaller channel thicknesses. The analysis focuses on comparing the 2 mm and 5 mm channels, where the highest temperatures are observed at the bottom of the heat sink above the electronic chip. The temperature profiles indicate that the 2 mm channel reaches higher maximum temperatures (40˚C to 56˚C) compared to the 5 mm channel (36˚C to 48˚C), primarily due to the thinner channel's reduced surface area for heat dissipation and increased localized heat accumulation. Although the 2 mm channel experiences intense convective heat transfer, its restricted flow velocity limits the nanofluid's heat removal capability.

Conversely, the 5 mm channel benefits from improved fluid circulation and heat transfer, resulting in a more balanced thermal environment and a lower temperature gradient. In a comparative analysis of pressure drop across various channel sizes in MCHS, it was observed that all nanofluids in the 2 mm channel outperform water, exhibiting the lowest pressure drop, which suggests superior flow behavior and reduced resistance. As channel size increases to 5 mm, both SiO_2 and ZnO nanofluids continue to maintain relatively low pressure drops, indicating their effectiveness in enhancing fluid flow, albeit with a slight increase in resistance due to larger cross-sectional area and potential turbulence. Conversely, in the 8 mm channel, all tested nanofluids experience higher pressure drops compared to the smaller channels, demonstrating the challenges of sustaining efficient flow in larger diameters. Notably, ZnO stands out as the

DOI: https://doi.org/10.22452/mjs.vol45sp1.1
Malaysian Journal of Science 45 (Special Issue 1): 1-10 (June 2026)

Table 6. Temperature and pressure surface of 2mm channel thickness from 2D YZ-cut plane.

Nanofluids	Temperature (°C)	Pressure (Pa)
Al_2O_3	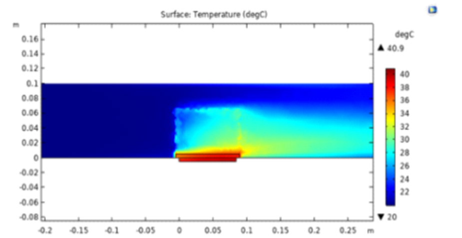	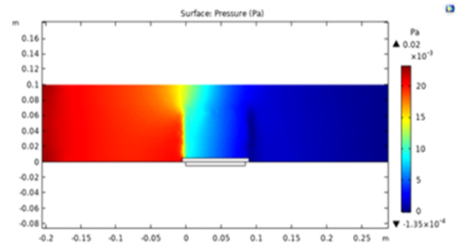
SiO_2	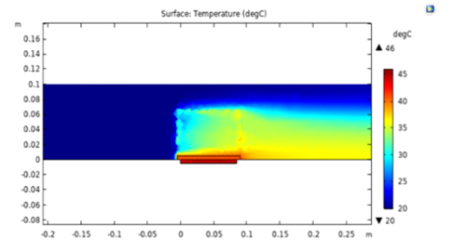	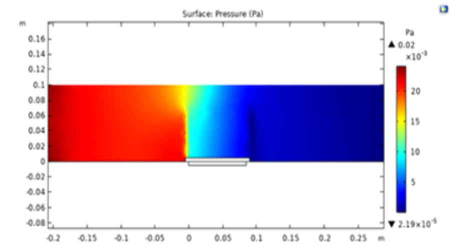
ZnO	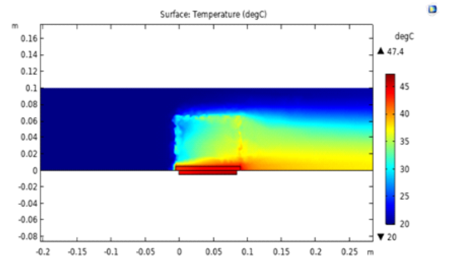	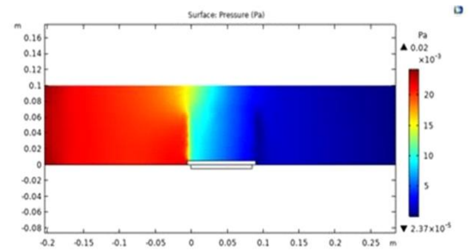
Air	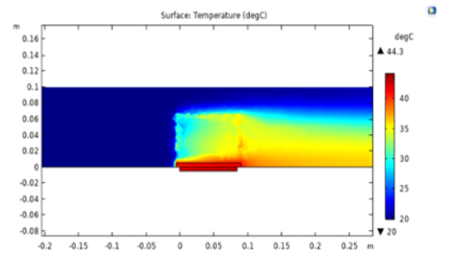	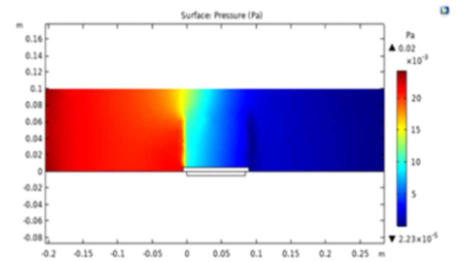
Water	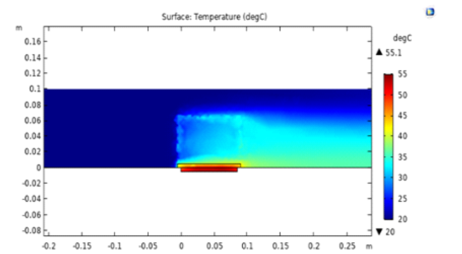	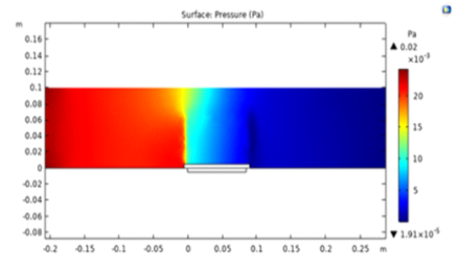

only nanofluid that retains a low pressure drop in this context, indicating its unique characteristics may help maintain flow efficiency under increased channel size. Overall, these results illustrate that the 2 mm channel, particularly when using nanofluids, provides the most effective option for minimizing pressure drop.

The measurements of channel thickness and coolant results were taken from -0.2 m (inlet) to 0.2 m (outlet), with the midpoint at 0 m along the x-axis. Overall, the lowest temperature was observed at the inlet, while the highest temperature occurred in the middle section. As the heat moved towards the outlet, the temperature decreased. The findings are detailed in Table 8, which analyzes the data for each channel thickness and nanofluid.

The results indicate that the 5 mm channel thickness achieves the lowest maximum temperature in the middle section, likely due to enhanced heat transfer and a more balanced flow distribution, allowing the coolant to absorb heat more effectively.

In contrast, the 2 mm channel thickness exhibits the lowest pressure drop, suggesting faster fluid velocity but potentially less time for effective heat absorption. This illustrates a trade-off between thermal efficiency and pressure loss, which is essential for optimizing heat sink designs based on specific cooling requirements.

DOI: https://doi.org/10.22452/mjs.vol45sp1.1
Malaysian Journal of Science 45 (Special Issue 1): 1-10 (June 2026)

Table 7. Temperature and pressure surface of 5mm channel thickness from 2D YZ-cut plane view.

Nanofluids	Temperature (℃)	Pressure (Pa)
Al_2O_3	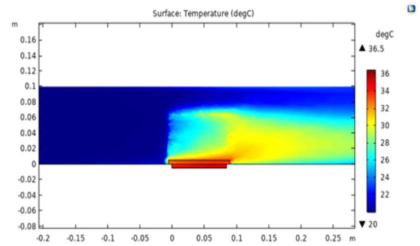	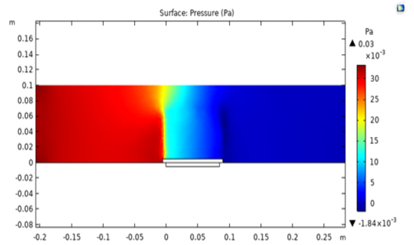
SiO_2	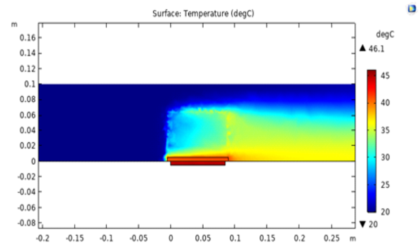	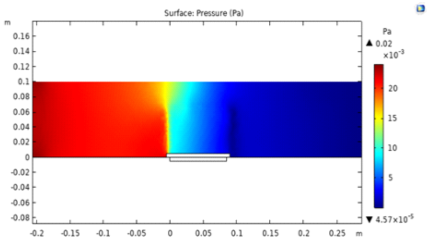
ZnO	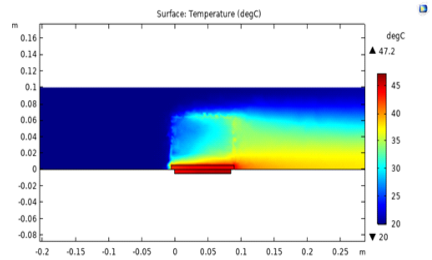	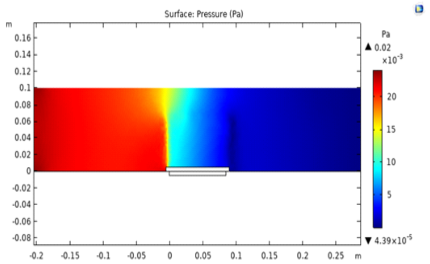
Air	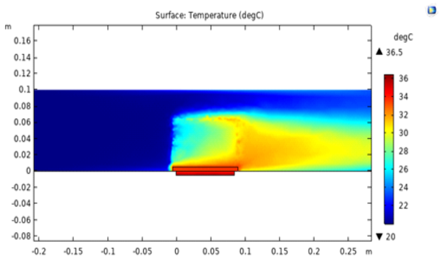	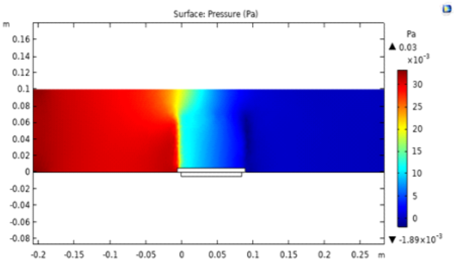
Water	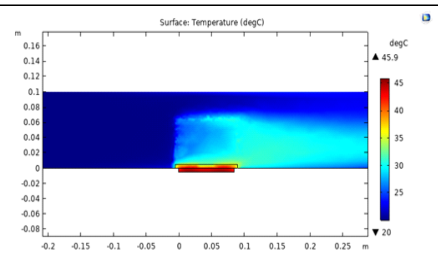	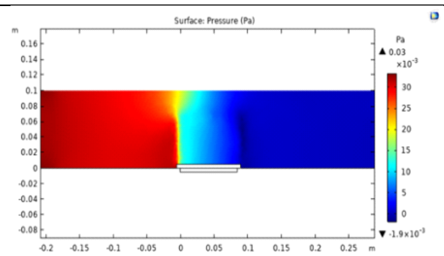

3.2 The effect of channel thickness on pressure drop

Measurements of different channel thicknesses and coolant temperature were taken from -0.2 m (inlet) to 0.2 m (outlet), with the midpoint at 0 m along the x-axis. The inlet exhibited the lowest temperature, while the maximum was observed in the middle section, gradually decreasing toward the outlet. Detailed results for each channel thickness and nanofluid are presented in Table 8.

Table 8 (a) shows that Al_2O_3 nanofluids have the lowest surface temperature and pressure drop due to their superior thermal conductivity, which improves heat transfer and reduces thermal resistance. This results in significantly lower surface temperatures compared with other nanofluids, as seen in the balanced temperature and pressure drop behavior. The high heat flux, combined with fast-moving Al_2O_3 nanofluids, raises the outlet temperature but allows effective heat dissipation along the channel. The low pressure drop observed suggests that Al_2O_3 nanofluids maintain stable flow dynamics, making them more effective at extracting heat and managing temperature in the MCHS. Other nanofluids, though subjected to the same conditions, show less efficient heat management, maintaining higher surface temperatures and larger thermal gradients, particularly near the channel outlet.

DOI: https://doi.org/10.22452/mjs.vol45sp1.1
Malaysian Journal of Science 45 (Special Issue 1): 1-10 (June 2026)

Table 8. Graph of surface temperature and pressure drops of different channel thicknesses in different nanofluids.

	Temperature (℃)	Pressure (Pa)
a) 2mm channel thickness	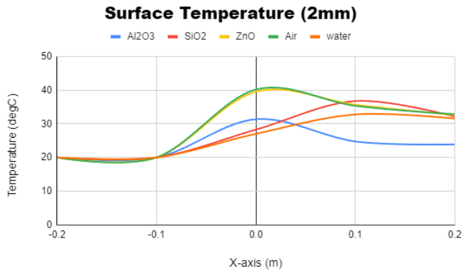	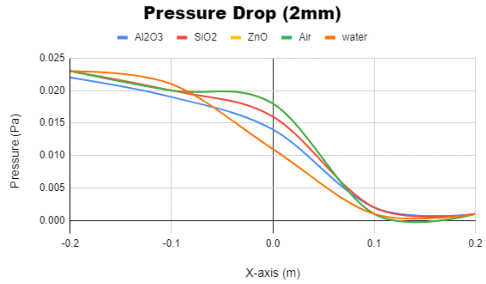
b) 5mm channel thickness	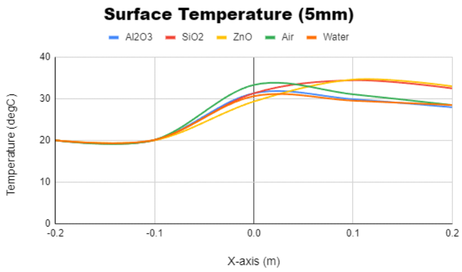	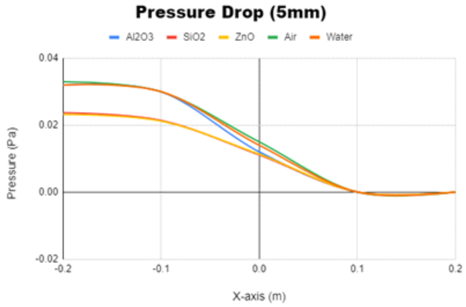
c) 8mm channel thickness	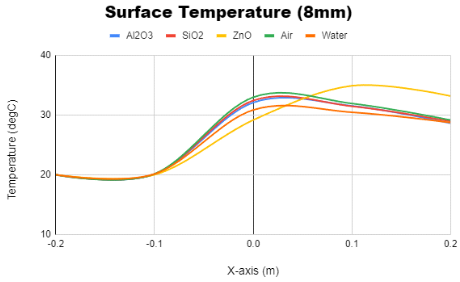	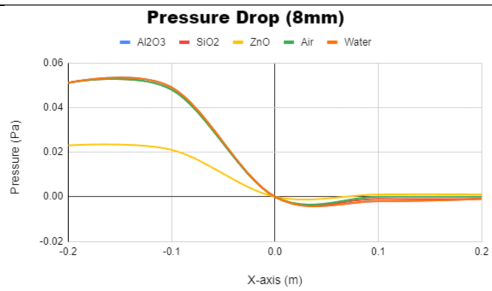

In Table 8 (b), point out the graphs for surface temperature and pressure drop of a 5 mm channel thickness. Al_2O_3 continues to exhibit the lowest surface temperature, indicating better heat transfer due to its high thermal conductivity. ZnO, in contrast, shows the highest surface temperature, reflecting less efficient heat dissipation. Al_2O_3 maintains low temperatures throughout, followed by water, air, and SiO_2, with ZnO performing the least effectively. When examining the pressure drop, air experiences the highest pressure drop, while ZnO has the lowest. The higher pressure drop observed for air flow is attributed to its low viscosity and compressibility, which increase flow resistance within the microchannel, rather than its density. All fluids show a zero pressure drop after exiting the MCHS, as the channel thickness affects fluid velocity, with a larger channel increasing resistance and thus the pressure drop within the MCHS.

Table 8 (c) shows the surface temperature and pressure drop for an 8 mm channel thickness. The temperature for this case indicates that there is no significant difference compared to the 5 mm channel thickness. However, in the 8 mm channel, the pressure drop is higher for all nanofluids except ZnO. The higher pressure drop in the 8 mm channel is likely due to increased friction from the larger surface area that contacts the fluid. Although the parabolic inlet velocity profile reduces wall shear stress, the increased channel size leads to more fluid-wall interaction, increasing resistance. Nanoparticles contacting the walls further increase wall shear stress, slowing the flow and causing higher pressure drops.

4. Conclusion

The copper rectangular MCHS was successfully modeled using COMSOL Multiphysics 5.5, with a detailed analysis of temperature and pressure drop for various nanofluids across channel thicknesses of 2mm, 5mm, and 8mm. Al_2O_3 nanofluid consistently showed the lowest temperature and highest pressure drop relative to other nanofluids, with the 5mm channel emerging as the optimal design due to its balanced performance. Al_2O_3 in the 5mm channel achieved the lowest maximum temperature of 27.39˚C, attributed to its superior thermal conductivity and efficient heat transfer. The 2mm channel, while providing higher surface area for fluid interaction, recorded the highest temperature of 39.52˚C with ZnO nanofluid, demonstrating that narrower channels face difficulties with constrained fluid flow and reduced thermal efficiency.

In contrast, the 8mm channel had the lowest pressure drop, particularly with ZnO, but its larger size did not significantly improve heat transfer, as indicated by slightly higher temperatures. The air in the 5mm channel experienced the

DOI: https://doi.org/10.22452/mjs.vol45sp1.1
Malaysian Journal of Science 45 (Special Issue 1): 1-10 (June 2026)

highest pressure drop, indicating that fluid dynamics have a strong influence on both heat dissipation and resistance. These findings emphasize the importance of carefully selecting both the nanofluid and channel size to optimize cooling performance. Overall, the 5mm channel showed the best heat transfer performance, offering a balanced approach to both temperature reduction and pressure drop. To further enhance microchannel heat sink efficiency, future improvements could involve optimizing the aspect ratio of Al_2O_3 nanoparticles or testing alternative materials, such as aluminum or iron, for the microchannel. This could lead to even greater cooling performance in electronic applications.

Acknowledgement

This study was supported by the Ministry of Higher Education (MOHE) through Fundamental Research Grant Scheme (FRGS) (FRGS/1/2019/STG02/UTHM/02/1) and Universiti Tun Hussein Onn Malaysia (UTHM) through vote K173. The authors would also like to thank the Faculty of Applied Sciences and Technology, Universiti Tun Hussein Onn Malaysia for its support.

References

Ahmed, H. E., Salman, B. H., Kherbeet, A. S., & Ahmed, M. I. (2018). Optimization of thermal design of heat sinks: A review. *International Journal of Heat and Mass Transfer*, *118*, 129-153.

Alkasmoul, F. S., Asaker, M., Almogbel, A., & AlSuwailem, A. (2022). Combined effect of thermal and hydraulic performance of different nanofluids on their cooling efficiency in microchannel heat sink. *Case Studies in Thermal Engineering*, *30*, 101776.

Al-Rashed, A. A., Shahsavar, A., Entezari, S., Moghimi, M. A., Adio, S. A., & Nguyen, T. K. (2019). Numerical investigation of non-Newtonian water-CMC/CuO nanofluid flow in an offset strip-fin microchannel heat sink: thermal performance and thermodynamic considerations. *Applied Thermal Engineering*, *155*, 247-258.

Alsabery, A. I., Gedik, E., Chamkha, A. J., & Hashim, I. (2019). Effects of two-phase nanofluid model and localized heat source/sink on natural convection in a square cavity with a solid circular cylinder. *Computer Methods in Applied Mechanics and Engineering*, *346*, 952-981.

Behnampour, A., Akbari, O. A., Safaei, M. R., Ghavami, M., Marzban, A., Shabani, G. A. S., & Mashayekhi, R. (2017). Analysis of heat transfer and nanofluid fluid flow in microchannels with trapezoidal, rectangular and triangular shaped ribs. *Physica E: Low-Dimensional Systems and Nanostructures*, *91*, 15-31.

Cao, Y., Abbas, M., El-Shorbagy, M. A., Gepreel, K. A., Dahari, M., Badran, M. F., ... & Wae-hayee, M. (2022). Thermo-hydraulic performance in ceramic-made microchannel heat sinks with an optimum fin geometry. *Case Studies in Thermal Engineering*, *36*, 102230.

Chen, X., & Chen, Y. (2021). A review on modelling, simulation and experiment of thermal conductivity of nanofluids. *International Journal of Environmental Analytical Chemistry*, *101*(10), 1347-1362.

Choi, S. U., & Eastman, J. A. (1995). *Enhancing thermal conductivity of fluids with nanoparticles* (No. ANL/MSD/CP-84938; CONF-951135-29). Argonne National Lab. (ANL), Argonne, IL (United States).

Coşkun, T., & Çetkin, E. (2020). Heat transfer enhancement in a microchannel heat sink: nanofluids and/or micro pin fins. *Heat Transfer Engineering*, *41*(21), 1818-1828.

Dhaiban, H. T., & Hussein, M. A. (2020). The optimal design of heat sinks: A review. *Journal of applied and computational mechanics*, *6*(4), 1030-1043.

Dogonchi, A. S., & Ganji, D. D. (2016). Investigation of MHD nanofluid flow and heat transfer in a stretching/shrinking convergent/divergent channel considering thermal radiation. *Journal of Molecular Liquids*, *220*, 592-603.

Elbadawy, I., Alhajri, A., Doust, M., Almulla, Y., Fayed, M., Dinc, A., ... & Al-Kouz, W. (2023). Reliability of different nanofluids and different micro-channel configurations on the heat transfer augmentation. *Processes*, *11*(3), 652.

Gao, J., Hu, Z., Yang, Q., Liang, X., & Wu, H. (2022). Fluid flow and heat transfer in microchannel heat sinks: Modelling review and recent progress. *Thermal Science and Engineering Progress*, *29*, 101203.

Gunnasegaran, P., Shuaib, N. H., Mohammed, H. A., Jalal, M. A., & Sandhita, E. (2012). Heat transfer enhancement in microchannel heat sink using nanofluids. *Fluid Dynamics, Computational Modeling and Applications*, 287-326.

Hamilton, R. L., & Crosser, O. K. (1962). Thermal conductivity of heterogeneous two-component systems. *Industrial & Engineering chemistry fundamentals*, *1*(3), 187-191.

Iyengar, M., & Bar-Cohen, A. (1998). Optimization of vertical pin-fin heat sinks in natural convective heat transfer. In *International Heat Transfer Conference Digital Library*. Begel House Inc.

Jennings Jr, D., & Smith, S. (2020, October). Comparative Study of Effective Cooling in Microchannel Heat Sinks (MCHS) With Nanofluid and Hydrophobic Nanostructures Using Computational Fluid Dynamics. In *International Electronic Packaging Technical Conference and Exhibition* (Vol. 84041, p. V001T07A002). American Society of Mechanical Engineers.

Li, W., Xie, Z., Xi, K., Xia, S., & Ge, Y. (2021). Constructal optimization of rectangular microchannel heat sink with porous medium for entropy generation minimization. *Entropy*, *23*(11), 1528.

Li, W., Zhu, L., Ji, F., Yu, J., Jin, Y., & Wang, W. (2020, July). Optimization of Manifold Mmicrochannel Heat Sink Based on Equivalent Resistance Model. In *2020 19th IEEE Intersociety*

Conference on Thermal and Thermomechanical Phenomena in Electronic Systems (ITherm) (pp. 497-500). IEEE.

Li, X., & Chen, J. (2019). Microembossed copper microchannel heat sink for high-density cooling in electronics. *Micro & Nano Letters*, *14*(12), 1258-1262.

Liou, T. M., Chang, S. W., & Chan, S. P. (2018). Effect of rib orientation on thermal and fluid-flow features in a two-pass parallelogram channel with abrupt entrance. *International Journal of Heat and Mass Transfer*, *116*, 152-165.

Littmarck, H. S., & Saeidi, F. (1986). Comsol. *COMSOL. Available: https://www. comsol. com/.,(accessed Aug. 1, 2022)*.

Malvandi, A., & Ganji, D. D. (2014). Brownian motion and thermophoresis effects on slip flow of alumina/water nanofluid inside a circular microchannel in the presence of a magnetic field. *International Journal of Thermal Sciences*, *84*, 196-206.

Memon, S. A., Cheema, T. A., Kim, G. M., & Park, C. W. (2020). Hydrothermal investigation of a microchannel heat sink using secondary flows in trapezoidal and parallel orientations. *Energies*, *13*(21), 5616.

Mohammed, H. A., Gunnasegaran, P., & Shuaib, N. H. (2010). Heat transfer in rectangular microchannels heat sink using nanofluids. *International Communications in Heat and Mass Transfer*, *37*(10), 1496-1503.

Muneeshwaran, M., Srinivasan, G., Muthukumar, P., & Wang, C. C. (2021). Role of hybrid-nanofluid in heat transfer enhancement–A review. *International Communications in Heat and Mass Transfer*, *125*, 105341.

Nazzal, I. T., Salem, T. K., & Al Doury, R. R. J. (2021, February). Theoretical investigation of a pin fin heat sink performance for electronic cooling using different alloys materials. In *IOP Conference Series: Materials Science and Engineering* (Vol. 1094, No. 1, p. 012087). IOP Publishing.

Pak, B. C., & Cho, Y. I. (1998). Hydrodynamic and heat transfer study of dispersed fluids with submicron metallic oxide particles. *Experimental Heat Transfer an International Journal*, *11*(2), 151-170.

Patel, A. K., Bhuvad, S., & Rajput, S. P. S. (2019). Effects of nanofluid flow in micro channel heat sink for forced convection cooling of electronics device: a numerical simulation. *Int J Innov Technol Exploring Eng (IJITEE)*, *9*(2), 5230-5243.

Rafiq, M., Shafique, M., Azam, A., & Ateeq, M. (2021). Transformer oil-based nanofluid: The application of nanomaterials on thermal, electrical and physicochemical properties of liquid insulation-A review. *Ain Shams Engineering Journal*, *12*(1), 555-576.

Rajput, R. S. & Sahu, H. (2021). Investigation of different types of heat sink and their applications. *International Journal of Rubber Technology (IJRT), 6*(3), 105-109.

Shamsuddin, H. S., Estelle, P., Navas, J., Mohd-Ghazali, N., & Mohamad, M. (2021). Effects of surfactant and nanofluid on the performance and optimization of a microchannel heat sink. *International Journal of Heat and Mass Transfer*, *175*, 121336.

Sohel, M. R., Khaleduzzaman, S. S., Saidur, R., Hepbasli, A., Sabri, M. F. M., & Mahbubul, I. M. (2014). An experimental investigation of heat transfer enhancement of a minichannel heat sink using Al2O3–H2O nanofluid. *International Journal of Heat and Mass Transfer*, *74*, 164-172.

Song, J., Liu, F., Sui, Y., & Jing, D. (2021). Numerical studies on the hydraulic and thermal performances of trapezoidal microchannel heat sink. *International Journal of Thermal Sciences*, *161*, 106755.

Sur, A., & Gulia, V. (2022). A comprehensive review on microchannel heat exchangers, heat sink, and polymer heat exchangers: Current state of the art. *Frontiers in Heat and Mass Transfer (FHMT)*, *18*.

Tang, K., Lin, G., Guo, Y., Huang, J., Zhang, H., & Miao, J. (2023). Simulation and optimization of thermal performance in diverging/converging manifold microchannel heat sink. *International Journal of Heat and Mass Transfer*, *200*, 123495.

Tuckerman, D. B., & Pease, R. F. W. (1981). High-performance heat sinking for VLSI. *IEEE Electron device letters*, *2*(5), 126-129.

Van Oevelen, T. (2014). Optimal heat sink design for liquid cooling of electronics.

Waqas, H., Khan, S. A., Farooq, U., Muhammad, T., Alshehri, A., & Yasmin, S. (2022). Thermal transport analysis of six circular microchannel heat sink using nanofluid. *Scientific Reports*, *12*(1), 8035.

Zhang, J., Guo, W., Xie, Z., Guan, X., Qu, X., & Ge, Y. (2023). Optimization of fin layout in liquid-cooled microchannels for multi-core chips. *Case Studies in Thermal Engineering*, *41*, 102615.

.

DOI: https://doi.org/10.22452/mjs.vol45sp1.1
Malaysian Journal of Science 45 (Special Issue 1): 1-10 (June 2026)